

On Similarity of Seismo Magnetic Field and Pressure Head Fractal Dimension for Characterizing Shajara Reservoirs of the Permo-Carboniferous Shajara Formation, Saudi Arabia

Khalid Elyas Mohamed Elameen Alkhidir

Department of Petroleum and Natural Gas Engineering, College of Engineering, King Saud University, Saudi Arabia

Corresponding author

Prof. Khalid Elyas Mohamed Elameen Alkhidir, Ph.D. Department of Petroleum and Natural Gas Engineering, College of Engineering, King Saud University, Saudi Arabia

Submitted: 28 Jan 2020; Accepted: 04 Feb 2020; Published: 15 Feb 2020

Abstract

The quality and assessment of a reservoir can be documented in details by the application of seismo magnetic field. This research aims to calculate fractal dimension from the relationship among seismo magnetic field, maximum seismo magnetic field and wetting phase saturation and to approve it by the fractal dimension derived from the relationship among inverse pressure head * pressure head and wetting phase saturation. Two equations for calculating the fractal dimensions have been employed. The first one describes the functional relationship between wetting phase saturation, seismo magnetic field, maximum seismo magnetic field and fractal dimension. The second equation implies to the wetting phase saturation as a function of pressure head and the fractal dimension. Two procedures for obtaining the fractal dimension have been utilized. The first procedure was done by plotting the logarithm of the ratio between seismo magnetic field and maximum seismo magnetic field versus logarithm wetting phase saturation. The slope of the first procedure = $3 - D_f$ (fractal dimension). The second procedure for obtaining the fractal dimension was determined by plotting the logarithm (inverse of pressure head and pressure head) versus the logarithm of wetting phase saturation. The slope of the second procedure = $D_f - 3$. On the basis of the obtained results of the fabricated stratigraphic column and the attained values of the fractal dimension, the sandstones of the Shajara reservoirs of the Shajara Formation were divided here into three units.

Keywords: Shajara Reservoirs, Shajara Formation, Seismo magnetic field fractal dimension, Pressure head fractal dimension, Permeability.

Introduction

Seismo electric effects related to electro kinetic potential, dielectric permittivity, pressure gradient, fluid viscosity, and electric conductivity was first reported by [1]. Capillary pressure follows the scaling law at low wetting phase saturation was reported by [2]. Seismo electric phenomenon by considering electro kinetic coupling coefficient as a function of effective charge density, permeability, fluid viscosity and electric conductivity was reported by [3]. The magnitude of seismo electric current depends on porosity, pore size, zeta potential of the pore surfaces, and elastic properties of the matrix was investigated by [4]. The tangent of the ratio of converted electric field to pressure is approximately in inverse proportion to permeability was studied by [5]. Permeability inversion from seism electric log at low frequency was studied by [6]. They reported that, the tangent of the ratio among electric excitation intensity and pressure field is a function of porosity, fluid viscosity, frequency, tortuosity and fluid density and Darcy permeability. A decrease

of seismo electric frequencies with increasing water content was reported by [7]. An increase of seismo electric transfer function with increasing water saturation was studied by [8]. An increase of dynamic seismo electric transfer function with decreasing fluid conductivity was described by [9]. The amplitude of seismo electric signal increases with increasing permeability which means that the seismo electric effects are directly related to the permeability and can be used to study the permeability of the reservoir was illustrated by [10]. Seismo electric coupling is frequency dependent and decreases exponentially when frequency increases was demonstrated by [11]. An increase of permeability with increasing seismo magnetic moment and seismo diffusion coefficient fractal dimension was reported by [12, 13]. An increase of, molar enthalpy, work, electro kinetic, bubble pressure and pressure head fractal dimensions with permeability increasing and grain size was described by [14, 15, 16, 17].

Material and Method

Sandstone samples were collected from the surface type section of the Permo-Carboniferous Shajara Formation, latitude $26^{\circ} 52' 17.4''$, longitude $43^{\circ} 36' 18''$. (Figure1). Porosity was measured on collected samples using mercury intrusion Porosimetry and permeability was

derived from capillary pressure data. The purpose of this paper is to obtain seismo magnetic field fractal dimension and to confirm it by pressure head fractal dimension. The fractal dimension of the first procedure is determined from the positive slope of the plot of logarithm of the ratio of seismo magnetic field to maximum seismo magnetic field $\log(H^{1/4}/H_{max}^{1/4})$ versus log wetting phase saturation (log Sw). Whereas the fractal dimension of the second procedure is determined from the negative slope of the plot of logarithm of log (inverse of pressure head α * pressure head h, $\log(\alpha * h)$ versus logarithm of wetting phase saturation (log Sw). The Seismo magnetic field can be scaled as

$$Sw = \left[\frac{H^{\frac{1}{4}}}{H_{max}^{\frac{1}{4}}} \right]^{[3-Df]} \quad (1)$$

Where Sw the water saturation, H the seismo magnetic field in ampere / meter, H_{max} the maximum seismo magnetic field in ampere / meter, and Df the fractal dimension. Equation 1 can be proofed from

$$H = \left[\frac{SEC}{d} \right] \quad (2)$$

Where H the seismo magnetic field in ampere / meter, SEC the seismo electric current in ampere, d the distance in meter. The seismo electric current SEC can be scaled as

$$SEC = \left[\frac{SEP}{R} \right] \quad (3)$$

Where SEC the seismo electric current in ampere, SEP the seismo electric potential in volt and R the resistance in ohm. Insert equation 3 into equation 2

$$H = \left[\frac{SEP}{d * R} \right] \quad (4)$$

The seismo electric potential SEP can be scaled as

$$SEP = \left[\frac{SEE}{q} \right] \quad (5)$$

Where SEP the seismo electric potential in volt, SEE the seismo electric energy in Joule, q the electric charge in coulomb. Insert equation 5 into equation 4

$$H = \left[\frac{SEE}{d * R * q} \right] \quad (6)$$

The seismo electric energy SEE can be scaled as

$$SEE = P * V \quad (7)$$

Where SEE the seismo electric energy in Joule, P the pressure in Pascal, and V the fluid volume in cubic meter. Insert equation 7 into equation 6

$$H = \left[\frac{P * V}{d * R * q} \right] \quad (8)$$

The Volume V can be scaled as

$$V = Q * t \quad (9)$$

Where V the volume in cubic meter, Q the flow rate in cubic meter / second and t the time in second. Insert equation 9 into equation 8

$$H = \left[\frac{P * Q * t}{d * R * q} \right] \quad (10)$$

The flow rate can be scaled as

$$Q = \left[\frac{3.14 * r^4 * \Delta P}{8 * \mu * L} \right] \quad (11)$$

Where Q the flow rate in cubic meter / second, r the pore radius in meter, ΔP the differentia pressure in Pascal, μ the fluid viscosity in Pascal * second, and L the capillary length in meter. Insert equation 11 into equation 10

$$H = \left[\frac{P * 3.14 * r^4 * \Delta P * t}{8 * d * R * q * \mu * L} \right] \quad (12)$$

The maximum pore radius r_{max} can be scaled as

$$H_{max} = \left[\frac{P * 3.14 * r_{max}^4 * \Delta P * t}{8 * d * R * q * \mu * L} \right] \quad (13)$$

Divide equation 12 by equation 13

$$\left[\frac{H}{H_{max}} \right] = \left[\frac{\left[\frac{P * 3.14 * r^4 * \Delta P * t}{8 * d * R * q * \mu * L} \right]}{\left[\frac{P * 3.14 * r_{max}^4 * \Delta P * t}{8 * d * R * q * \mu * L} \right]} \right] \quad (14)$$

Equation 14 after simplification will become

$$\left[\frac{H}{H_{max}} \right] = \left[\frac{r^4}{r_{max}^4} \right] \quad (15)$$

Take the fourth root of equation 15

$$\sqrt[4]{\left[\frac{H}{H_{max}} \right]} = \sqrt[4]{\left[\frac{r^4}{r_{max}^4} \right]} \quad (16)$$

Equation 16 after simplification will become

$$\left[\frac{H^{\frac{1}{4}}}{H_{max}^{\frac{1}{4}}} \right] = \left[\frac{r}{r_{max}} \right] \quad (17)$$

Take the logarithm of equation 17

$$\log \left[\frac{H^{\frac{1}{4}}}{H_{max}^{\frac{1}{4}}} \right] = \log \left[\frac{r}{r_{max}} \right] \quad (18)$$

$$\text{But; } \log \left[\frac{r}{r_{max}} \right] = \left[\frac{\log Sw}{3 - Df} \right] \quad (19)$$

Insert equation 19 into equation 18

$$\left[\frac{\log Sw}{3 - Df} \right] = \log \left[\frac{H^{\frac{1}{4}}}{H_{\max}^{\frac{1}{4}}} \right] \quad (20)$$

Equation 20 after log removal will become

$$Sw = \left[\frac{H^{\frac{1}{4}}}{H_{\max}^{\frac{1}{4}}} \right]^{[3-Df]} \quad (21)$$

Equation 21 the proof of equation 1 which relates the water saturation, seismo magnetic field, maximum seismo magnetic field, and the fractal dimension.

The pressure head can be scaled as

$$\text{LogSw} = [Df - 3] * \log(\alpha * h) + \text{constant} \quad (22)$$

Where Sw the water saturation, α inverse of pressure head, h the pressure head and Df the fractal dimension.

Results and Discussion

Based on field observation the Shajara Reservoirs of the Permo-Carboniferous Shajara Formation were divided here into three units as described in Figure 1. These units from bottom to top are: Lower Shajara Reservoir, Middle Shajara reservoir, and Upper Shajara Reservoir. Their attained results of the seismo magnetic field fractal dimension and pressure head fractal dimension are shown in Table 1. Based on the achieved results it was found that the seismo magnetic field fractal dimension is equal to the pressure head fractal dimension. The maximum value of the fractal dimension was found to be 2.7872 allocated to sample SJ13 from the Upper Shajara Reservoir as verified in Table 1. Whereas the minimum value of the fractal dimension 2.4379 was reported from sample SJ3 from the Lower Shajara reservoir as shown in Table 1. The Seismo magnetic field fractal dimension and pressure head fractal dimension were detected to increase with increasing permeability as proofed in Table 1 owing to the possibility of having interconnected channels.

The Lower Shajara reservoir was symbolized by six sandstone samples (Figure 1), four of which label as SJ1, SJ2, SJ3 and SJ4 were carefully chosen for capillary pressure measurement as proven in Table 1. Their positive slopes of the first procedure log of the Seismo magnetic field to maximum Seismo magnetic field versus log wetting phase saturation (Sw) and negative slopes of the second procedure log (inverse of pressure head α *pressure head h) versus log wetting phase saturation (Sw) are clarified in Figure 2, Figure 3, Figure 4, Figure 5 and Table 1. Their Seismo magnetic field fractal dimension and pressure head fractal dimension values are revealed in Table 1. As we proceed from sample SJ2 to SJ3 a pronounced reduction in permeability due to compaction was described from 1955 md to 56 md which reflects decrease in Seismo magnetic field fractal dimension from 2.7748 to 2.4379 as quantified in table 1. Again, an increase in grain size and permeability was proved from sample SJ4 whose seismo magnetic field fractal dimension and pressure head fractal dimension was found to be 2.6843 as described in Table 1.

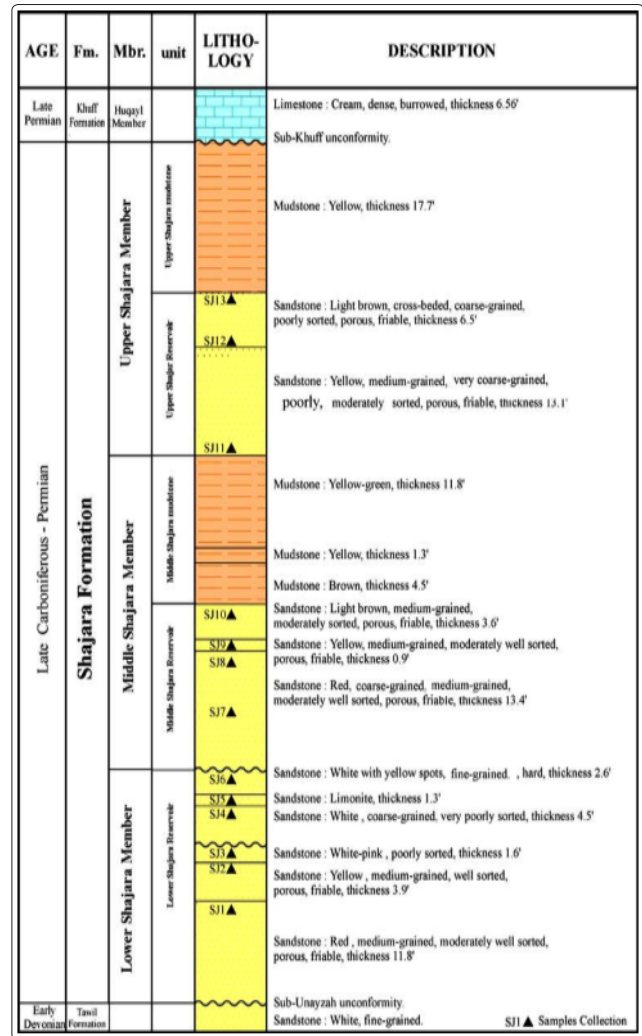


Figure 1: Surface type section of the Shajara Reservoirs of the Permo-Carboniferous Shajara Formation at latitude 26° 52' 17.4" longitude 43° 36' 18"

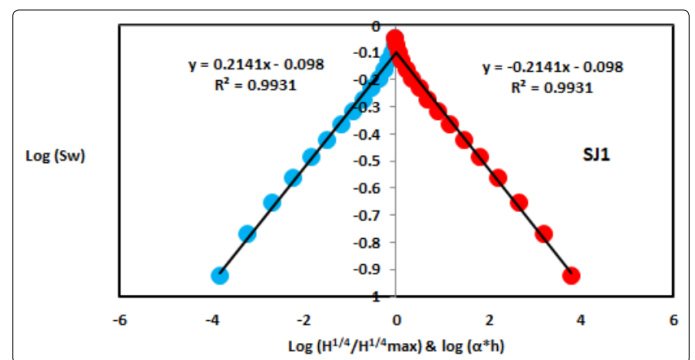


Figure 2: Log (H^{1/4}/H^{1/4}_{max}) & log (α * h) versus log Sw for sample SJ1

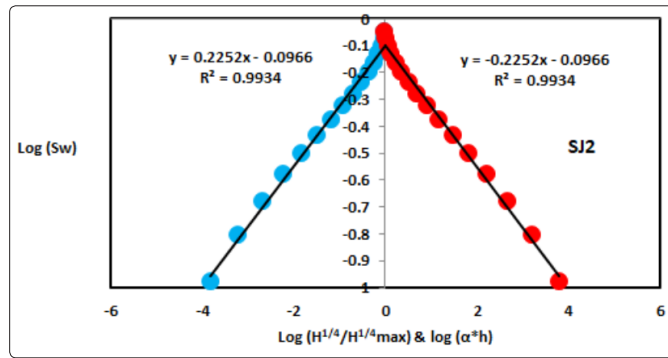


Figure 3: Log ($H^{1/4}/H^{1/4}_{max}$) & log ($\alpha * h$) versus log Sw for sample SJ2

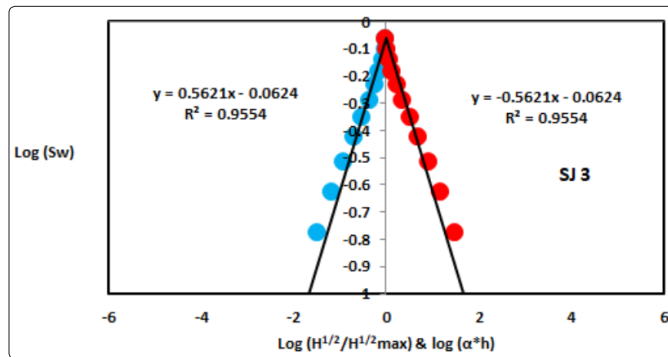


Figure 4: Log ($H^{1/2}/H^{1/2}_{max}$) & log ($\alpha * h$) versus log Sw for sample SJ3

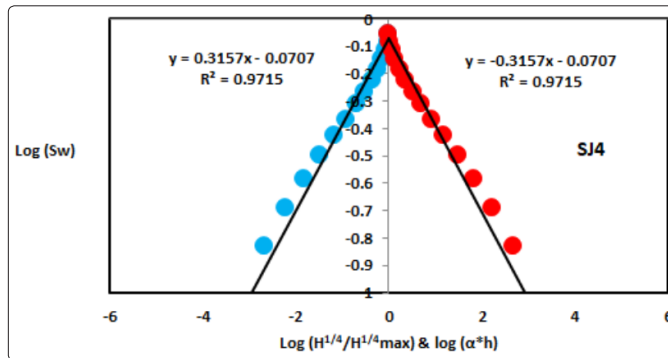


Figure 5: Log ($H^{1/4}/H^{1/4}_{max}$) & log ($\alpha * h$) versus log Sw for sample SJ4

Table 1: Petrophysical model showing the three Shajara Reservoir Units with their corresponding values of seismo magnetic fieldfractal dimension and pressure headfractal dimension

Table 1:	Reservoir	Sample	Porosity %	k (md)	Positive slope of the first procedure Slope=3-Df	Negative slope of the second procedure Slope=Df-3	Seismo magnetic field fractal dimension	Pressure head fractal dimension
Shajara Formation Permian-Carboniferous	Upper Shajara Reservoir	SJ13	25	973	0.2128	-0.2128	2.7872	2.7872
		SJ12	28	1440	0.2141	-0.2141	2.7859	2.7859
		SJ11	36	1197	0.2414	-0.2414	2.7586	2.7586
	Middle Shajara Reservoir	SJ9	31	1394	0.2214	-0.2214	2.7786	2.7786
		SJ8	32	1344	0.2248	-0.2248	2.7752	2.7752
		SJ7	35	1472	0.2317	-0.2317	2.7683	2.7683
	Lower Shajara Reservoir	SJ4	30	176	0.3157	-0.3157	2.6843	2.6843
		SJ3	34	56	0.5621	-0.5621	2.4379	2.4379
		SJ2	35	1955	0.2252	-0.2252	2.7748	2.7748
		SJ1	29	1680	0.2141	-0.2141	2.7859	2.7859

In contrast, the Middle Shajara reservoir which is separated from the Lower Shajara reservoir by an unconformity surface as revealed in Figure 1. It was nominated by four samples (Figure 1), three of which named as SJ7, SJ8, and SJ9 as illuminated in Table 1 were chosen for capillary measurements as described in Table 1. Their positive slopes of the first procedure and negative slopes of the second procedure are shown in Figure 6, Figure 7 and Figure 8 and Table 1. Furthermore, their Seismo magnetic field fractal dimensions and pressure head fractal dimensions show similarities as defined in Table 1. Their fractal dimensions are higher than those of samples SJ3 and SJ4 from the Lower Shajara Reservoir due to an increase in their permeability as explained in table 1.

On the other hand, the Upper Shajara reservoir was separated from the Middle Shajara reservoir by yellow green mudstone as shown in Figure 1. It is defined by three samples so called SJ11, SJ12, SJ13 as explained in Table 1. Their positive slopes of the first procedure and negative slopes of the second procedure are displayed in Figure 9, Figure 10 and Figure 11 and Table 1. Moreover, their seismo magnetic field fractal dimension and pressure head fractal dimension are also higher than those of sample SJ3 and SJ4 from the Lower Shajara Reservoir due to an increase in their permeability as simplified in table 1.

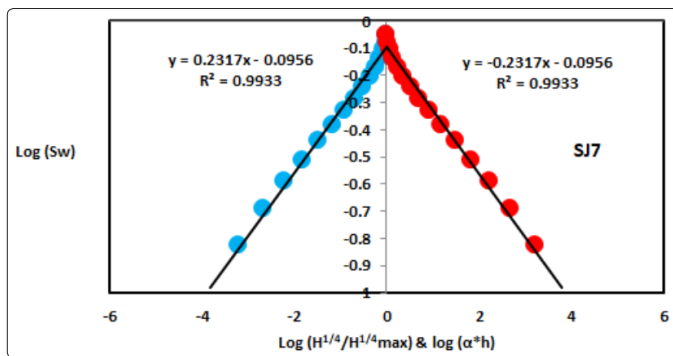


Figure 6: Log ($H^{1/4}/H^{1/4max}$) & log ($\alpha * h$) versus log Sw for sample SJ7

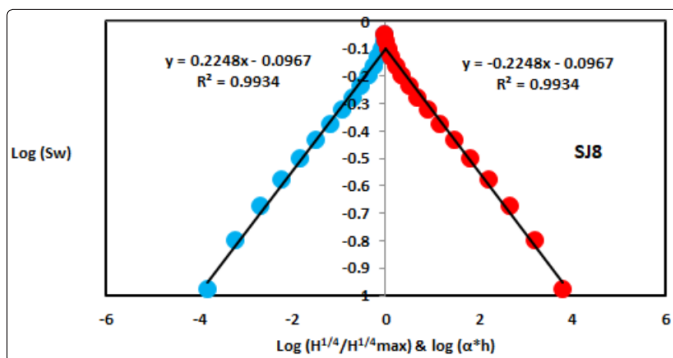


Figure 7: Log ($H^{1/4}/H^{1/4max}$) & log ($\alpha * h$) versus log Sw for sample SJ8

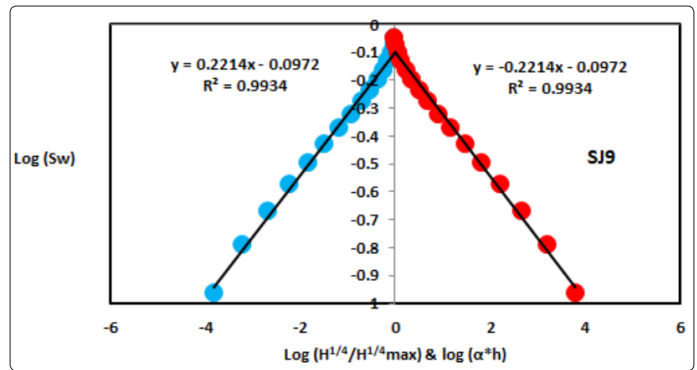


Figure 8: Log ($H^{1/4}/H^{1/4max}$) & log ($\alpha * h$) versus log Sw for sample SJ9

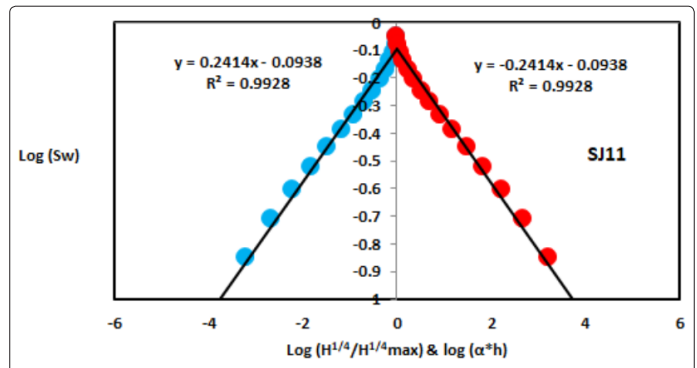


Figure 9: Log ($H^{1/4}/H^{1/4max}$) & log ($\alpha * h$) versus log Sw for sample SJ11

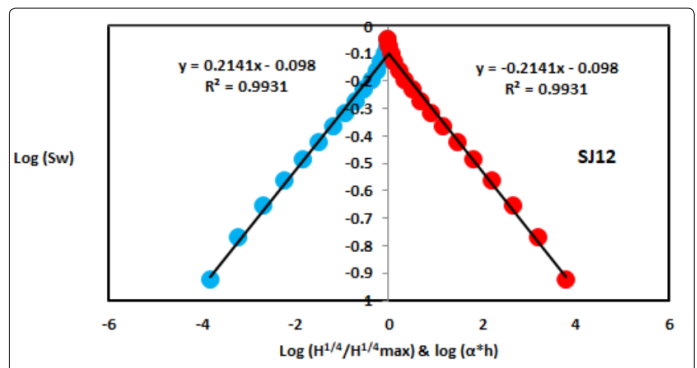


Figure 10: Log ($H^{1/4}/H^{1/4max}$) & log ($\alpha * h$) versus log Sw for sample SJ12

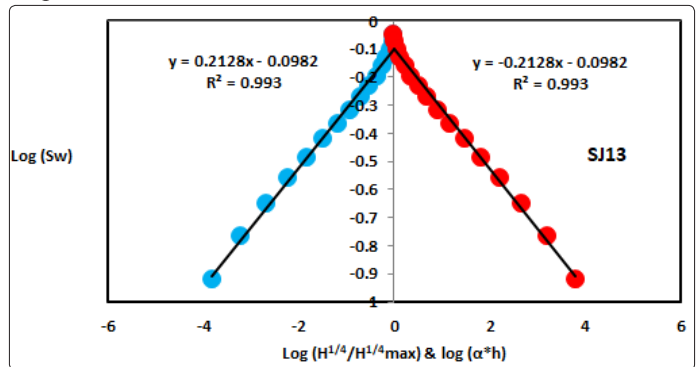


Figure 11: Log ($H^{1/4}/H^{1/4max}$) & log ($\alpha * h$) versus log Sw for sample SJ13

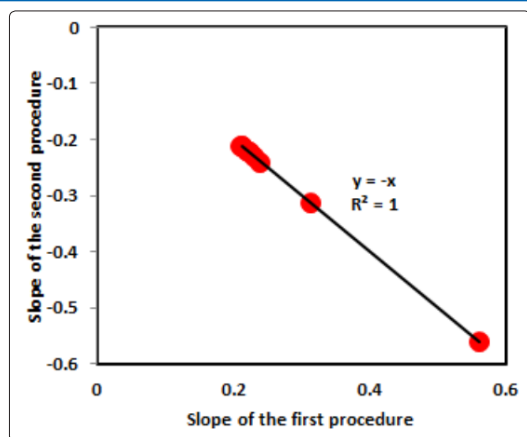


Figure 12: Slope of the first procedure versus slope of the second procedure

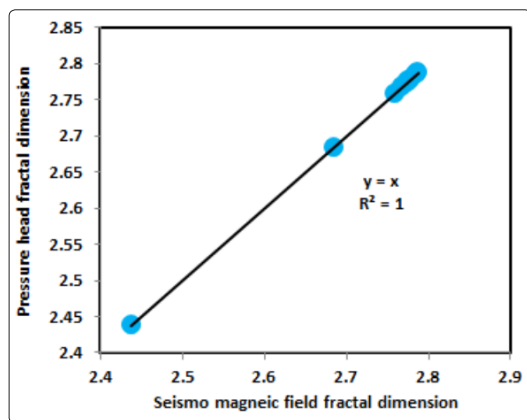


Figure 13: Seismo magnetic field fractal dimension versus pressure head fractal dimension

Conclusion

The sandstones of the Shajara Reservoirs of the permo-Carboniferous Shajara Formation were divided here into three units based on seismo magnetic field fractal dimension. The Units from base to top are: Lower Shajara Seismo Magnetic Field Fractal Dimension Unit, Middle Shajara Seismo Magnetic Field Fractal Dimension Unit, and Upper Shajara Seismo Magnetic Field Fractal Dimension Unit. These units were also proved by pressure head fractal dimension. The fractal dimension was found to increase with increasing grain size and permeability owing to possibility of having interconnected channels.

Acknowledgement

The author would to thank King Saud University, college of Engineering, Department of Petroleum and Natural Gas Engineering, Department of Chemical Engineering, Research Centre at College of Engineering, College of science, Department of Geology, and King Abdullah Institute for research and Consulting Studies for their supports.

References

1. Frenkel J (1944) on the theory of seismic and seismo electric phenomena in a moist soil. *Journal of physics* 3: 230-241.
2. Li K, Williams W (2007) Determination of pressure head function from resistivity data. *Transport in Porous Media* 67: 1-15.

3. Revil A, Jardani A (2010) Seismo electric response of heavy oil reservoirs: theory and numerical modelling. *Geophysical J International* 180: 781-797.
4. Dukhin A, Goetz P, Thommes M (2010) Seismo electric effect: a non-isochoric streaming current.1 Experiment. *J Colloid Interface Sci* 345: 547-553.
5. Guan W, Hu H, Wang Z (2012) Permeability inversion from low-frequency seismo electric logs in fluid- saturated porous formations. *Geophysics Prospect* 61: 120-133.
6. Hu H, Guan W, Zhao W (2012) Theoretical studies of permeability inversion from seismo electric logs. *Geophysical Research Abstracts* 14: EGU2012-6725-1 2012 EGU General Assembly.
7. Borde C, Sen echal P Barri`ere J, Brito D, Normandin E, et al. (2015) Impact of water saturation on seismo electric transfer functions: a laboratory study of co-seismic phenomenon. *Geophysical J International* 200: 1317-1335.
8. Jardani A, Revil A (2015) Seismo electric couplings in a poroelastic material containing two immiscible fluid phases. *Geophysical Journal International* 202: 850-870.
9. Holzhauer J, Brito D, Bordes C, Brun Y, Guatarbes B (2016) Experimental quantification of the seism electric transfer function and its dependence on conductivity and saturation in loose sand. *Geophysics Prospect* 65: 1097-1120
10. Rong Peng, Jian-Xing Wei, Bang-Rang Di, Pin-Bo Ding, ZiChun Liu, et al. (2016) Experimental research on seismo electric effects in sandstone. *Applied Geophysics* 13: 425-436.
11. Djuraev U, Jufar S R, Vasant P (2017) Numerical Study of frequency-dependent seismo electric coupling in partially saturated porous media. *MATEC Web of Conferences* 87: 02001.
12. Alkhidir KEME (2020) Seismo Magnetic Moment Fractal Dimension for Characterizing Shajara Reservoirs of the Permo Carboniferous Shajara Formation, Saudi Arabia *World Scientific News* 139: 186-200.
13. Alkhidir KEME (2019) Seismo Diffusion Coefficient Fractal Dimension for Characterizing Shajara Reservoirs of the Permo-Carboniferous Shajara Formation, Saudi Arabia. *Research Journal of Nano science and Engineering* 3: 23-29.
14. Alkhidir KEME (2019) Molar Enthalpy Fractal Dimension for Characterizing Shajara Reservoirs of the Permo-Carboniferous Shajara Formation. *Journal of Agriculture and Aquaculture* 1: 1-8.
15. Alkhidir KEME (2019) Work Fractal Dimension for Characterizing Shajara Reservoirs of the Permo Carboniferous Shajara Formation, Saudi Arabia. *Int J Environ & Agri Sci* 3: 1-8
16. Alkhidir KEME (2018) Electro Kinetic Fractal Dimension for Characterizing Shajara Reservoirs of the Shajara Formation. *Int J Nano Med & Eng.* 3: 54-60.
17. Al-Khidir KE (2018) On Similarity of Pressure Head and Bubble Pressure Fractal Dimensions for Characterizing Permo-Carboniferous Shajara Formation, Saudi Arabia. *J Indust Pollut Toxic* 1: 102.

Copyright: ©2020 Khalid Elyas Mohamed Elameen Alkhidir. This is an open-access article distributed under the terms of the Creative Commons Attribution License, which permits unrestricted use, distribution, and reproduction in any medium, provided the original author and source are credited.